Flood Infrastructure: Localized Scour at Piano Key Weirs

Wyatt Lantz, Graduate Researcher, Utah State University/Utah Water Research Laboratory;
Brian Crookston, PhD PE, Assistant Professor, Utah State University; and
Michele Palermo, PhD, Associate Professor, University of Pisa

Abstract— Historic growth in the US coupled with observed hydrologic changes have created an increased demand for sustainable flood protection. One approach to passing floodwaters is nonlinear weirs such as labyrinth and Piano Key weirs (PK weirs). Although they are being designed in greater frequency, one area lacking in information or design guidance is the prediction of local scour at these weirs. Without proper protection, downstream local scour can compromise the weirs' foundation. Therefore, a large-scale laboratory study has been undertaken to investigate the effect of different lengths of downstream aprons on the scour mechanism at the foundation of a PK weir. This paper presents a preliminary analysis of equilibrium scour morphology under different flow conditions and with non-cohesive bed material. Instrumentation included 3D cameras and ultrasonic sensors to capture scour features and measure dynamic water surface elevations, respectively.

I. INTRODUCTION

Three intense flooding periods occurred in succession in the USA from March through September in 2019. Areas most severely impacted were along the Arkansas, Mississippi, and Missouri Rivers in the Midwest and in southern States (Floodlist, 2020). Consequently, impacts were estimated to be about 14 million citizens affected by floodwaters, 92 flood fatalities, and over $10 billion in economic damages (NOAA 2020, Center for Disaster Philanthropy 2019). Unfortunately, 2019 was not a rare or isolated year; flooding consequences from past events indicated that future risks are increasing exponentially, exacerbated by population growth and climate change. Researchers at Princeton University recently concluded a study noting that many current 100-year flood event estimates are occurring three-times more frequently (Marsooli et al. 2019). As a result, there is significant interest in sustainable flood risk management (Green 2010).

Spillways and control structures are a critical component of dams, levees, and rivers systems and provide flood protection benefits. However, many hydraulic structures are older and require rehabilitation due to deterioration, hydraulic deficiencies, and evolving performance criteria. Although a variety of approaches are being implemented in response to flood infrastructure challenges, weirs are still widely and effectively used. For example, non-linear weirs are advantageous as control structures in rivers due to their hydraulic efficiency, passive nature, and ability to pass driftwood and other debris (Crookston et al. 2019). Local scour often occurs at hydraulic structures and in times of peak flows, the scour is often unwanted, excessive, or may even compromise functionality or stability of the structure leading to an incident or failure. For example, the labyrinth weir in the Brazos River, Texas provides great benefit to the adjacent communities but experienced scour downstream of the apron that was subsequently repaired with riprap (Vasquez et al. 2008).

Local scour undermining the foundation of a weir or stilling basin located in a river is a complex process, which depends on structure geometry, flow characteristics and duration, turbulence intensity and sediment properties. Many researchers have studied local scour in correspondence with different hydraulic structures (among others, Breusers and Raudkivi 1991, Hoffmans and Verheij 1997, Bormann and Julien 1991), focusing on scour due to jets (Adduce and Sciortino 2006, Bombardelli et al. 2018), scour at culverts (Abt et al. 1987), scour at weir-like structures (Wang et al. 2019) and scour at bridge piers (Laursen 1952, Chiew and Melville 1987). In particular, there are several studies dealing with scour at concrete linear weirs (e.g., Stein et al. 1993, D'Agostino and Ferro 2004) who attempted to predict scour at sharp-crested weirs but little is known regarding local scour at non-linear weirs (Jüstrich et al. 2016, Pfister et al. 2017, and Wang et al. 2019). Furthermore, scour information, guidance, and predictive methods directed towards practitioners are limited (ASCE Task Committee on Scour at Channel-control Structures, personal communication, 2020). With limited information it may be difficult to assess appropriate cutoff wall depths and any scour protection measures such as a concrete apron.

Therefore, in consideration of the increase in flooding frequency and the lack of scour information and guidance at non-linear weirs, a large-scale multi-phase laboratory study has been undertaken at Utah State University to investigate the local scour

This research was funded by the US Geologic Survey and the State of Utah through Utah State University.

processes downstream of a PK weir. Scour protection via downstream aprons of three different lengths were also investigated. This study is funded by the State of Utah, the US Geologic Survey, and is in collaboration with the University of Pisa, Italy and the University of California Davis. This paper presents the first results of Phase 1, involving a medium-sized or coarse gravel. The objectives of this study included:

- Quantifying the main scour features at equilibrium with and without a downstream apron
- Developing graphical relationships for scour inducing variables
- Providing results that would inform selection of foundation protection measures such as cutoff walls and downstream aprons

II. Experimental Setup

Experiments have been conducted in a 2-meter wide, 1.8-meter deep, 16-meter long flume (approximately 6.6 ft wide, 6 ft deep, 52 ft long) for discharges up to about 600 L/s (21 cfs). The PK weir is a 4-key (N=4) type A geometry with a height, P= 0.42 m (16.5 in.), inlet to outlet key ratio, W_i/W_o=1.28 with a flat crest (Figure 1). The height of PK foundation is 1.09 m (43 in.) to avoid any influence of the channel bottom on the scour process. Investigations included scenarios with no downstream protective apron (reference tests), and three different apron lengths (L_a). The aprons were fabricated from wood sheeting and included a downstream vertical face similar to a cutoff wall to prevent any undermining or scour beneath the apron. Gravel material was removed to place these aprons and then carefully levelled to obtain a horizontal bed. Note that a false floor was not included upstream of the PK weir to represent a theoretical river bottom. The temporal evolution of scour geometry, including maximum scour depth (Z_{max}), its longitudinal position from the PK weir (X_{Max}), and scour length (L), were carefully monitored (Figure 2). Tests were conducted using a non-cohesive gravel whose granulometric characteristics are d_{90} = 20mm (0.75 in.), d_{50} = 13 mm (0.5 in.), non-uniformity coefficient σ = 1.54, density ρ = 2604.28 kg/m^3 (5.05 slug/ft^3), specific weight γ = 25,539.3 N/m^3 (162.6 lb/ft^3), and specific gravity G = 2.60 where d_{xx} indicating the diameter of the bed material for which xx% is finer. Subsequent phases of this study will consider smaller gravel materials. The experimental test matrix is presented in Table 1.

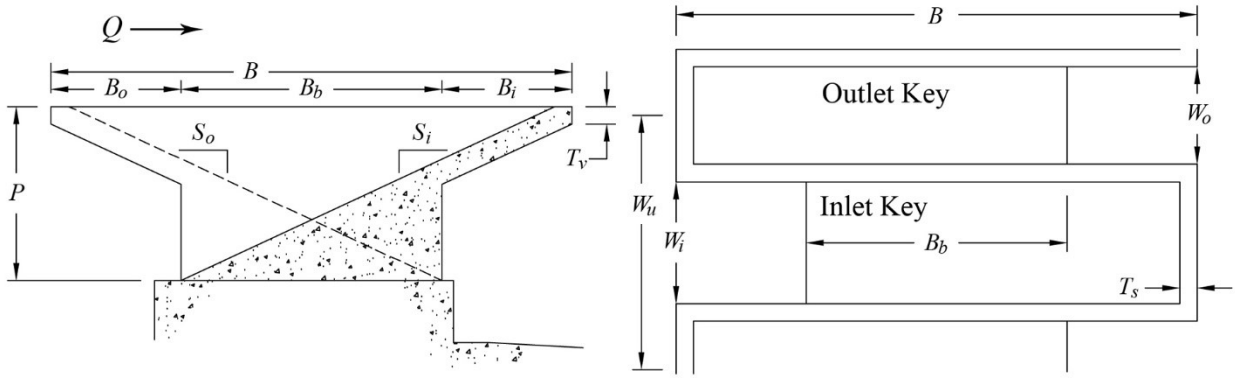

Figure 1. Overview of geometric parameters for a Type A PK weir (Crookston et al. 2016).

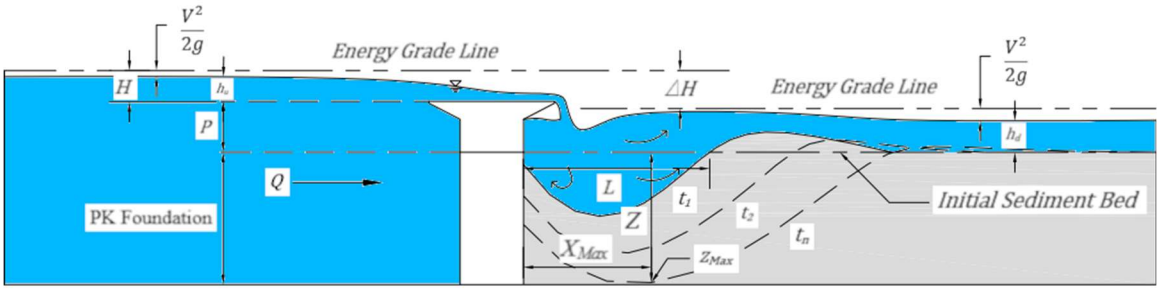

Figure 2. Schematic of geometrical and hydraulic parameters (reference test).

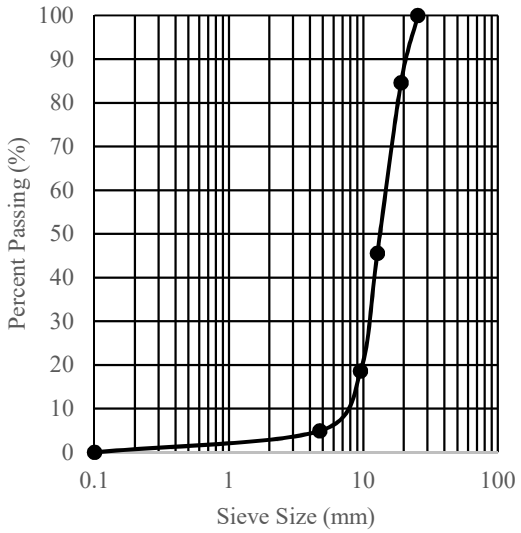

Figure 3. Sieve analysis for the gravel material studied herein.

Flow conditions upstream of the PK weir were established using a headbox with a diffuser and rock baffle. Total head (H) is defined as depth of flow above weir crest (h_u) plus the corresponding velocity head ($V^2/2g$). Tailwater was set using a stop log assembly. An experiment was performed by first slowly filling the flume with a high tailwater (submerged weir) and minimizing local velocities and shear stresses. Once the target flow rate was reached the stop logs were removed to set the desired tailwater elevation. Once upstream and downstream conditions were achieved the simulation timer began with the video camera array to document observations. A clear acrylic window in the right flume wall facilitated observations. Scour measurements were taken every few minutes during the first 30 minutes of an experiment due to rapid scour evolution. As time progressed and the rate of scour decreased, measurements were taken less frequently until the experiment was considered to be at quasi-equilibrium. A selection of tests were performed for more than 18 hrs where it was observed that equilibrium conditions had been achieved; this facilitated the selection of appropriate experiment durations to investigate scour morphology with and without a downstream apron.

Discharges were measured using a calibrated venturi meter (±0.25%). Upstream water surface elevations were measured using a stilling well. Ultrasonic sensors (Microsonic mic+130/IU/TC) were also used to measure the dynamic water surface profile within the flume. A simple technique was employed to estimate the temporal evolution of local scour. Small buoyant spheres were placed in the substrate at precise elevations forming vertical columns; as the substrate was eroded and a sphere was exposed, it was removed and quickly rose to the surface. The specific weight of the spheres was controlled to allow the spheres to rise to the surface without being prematurely removed due to a strong buoyancy force. Figure 4 shows the sphere locations for the reference scenario. As an apron was added spheres were moved the corresponding apron length downstream.

Following each test, an Intel-RealSense stereo imaging camera was used to scan the downstream bed topography (±1 mm accuracy) and quantify the final dimensions of the scour hole. Camera images are post-processed using a program written in MATLAB to gather various scour dimensions and to generate various plots of 2D and 3D scour profiles and maximum scour features as a function of discharge and tailwater.

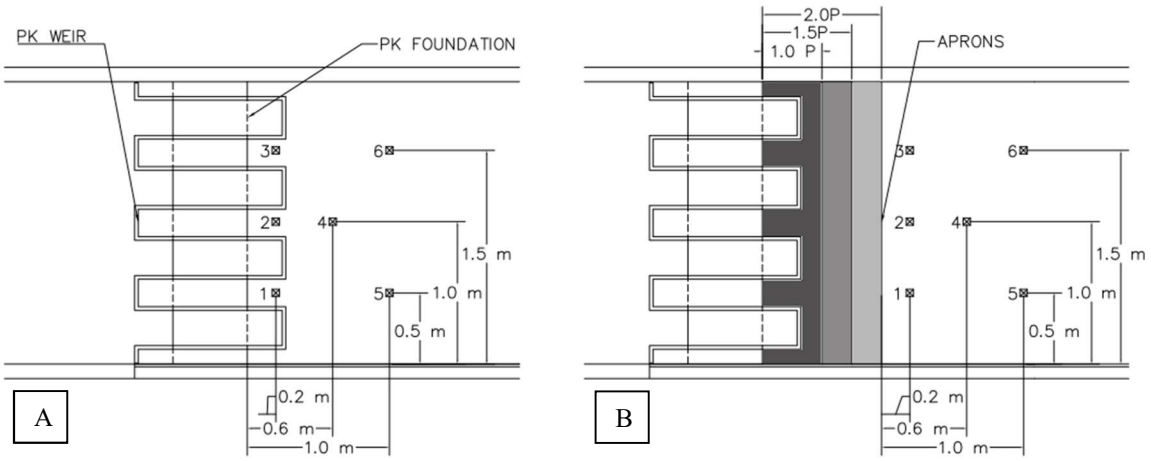

Figure 4. Sphere location for (A) reference test and (B) tests with aprons.

Table 1. Test matrix for this study.

Discharge	Headwater	Tailwater	Apron Length
150 L/s	*H/P*~0.11	0.3*P*~14 cm	2.0*P*
			1.5*P*
			1.0*P*
			0.0*P*
		0.6*P*~28 cm	0.0*P*
		0.9*P*~42 cm	0.0*P*
300 L/s	*H/P*~0.18	0.3*P*~14 cm	2.0*P*
			1.5*P*
			1.0*P*
			0.0*P*
		0.6*P*~28 cm	0.0*P*
		0.9*P*~42 cm	0.0*P*
600 L/s	*H/P*~0.35	0.3*P*~14 cm	2.0*P*
			1.5*P*
			1.0*P*
			0.0*P*
		0.6*P*~28 cm	0.0*P*
		0.9*P*~42 cm	0.0*P*

III. RESULTS

Hydraulics

Scour at the foundation or toe of the PK weir are deeply influenced by hydraulic characteristics of the structure. The flow varies across the width of the structure due to the inlet and outlet keys. Thus, this weir produces two types of impinging jets, i.e., vertical and oblique jets, as shown in Figure 5. Vertical (or sub-vertical) jets originate from the inlet keys and are characterized by a reduced horizontal component of the momentum flux. The remaining flow cascading over the weir crest does not fall downstream of the weir but into the sloping outlet keys. Therefore, flows from the portion of crest along the outlet keys are combined into angled jets. Notably, a flow discharge concentration occurs at the outlet keys, resulting in an increase of local shear stresses acting on the granular bed. Therefore, a greater maximum scour depth is caused by higher unit jet power at the outlet keys. These observations also indicate that the depth of a PK weir (*B*) and the corresponding weir crest length are significant parameters influencing maximum scour downstream of a PK weir.

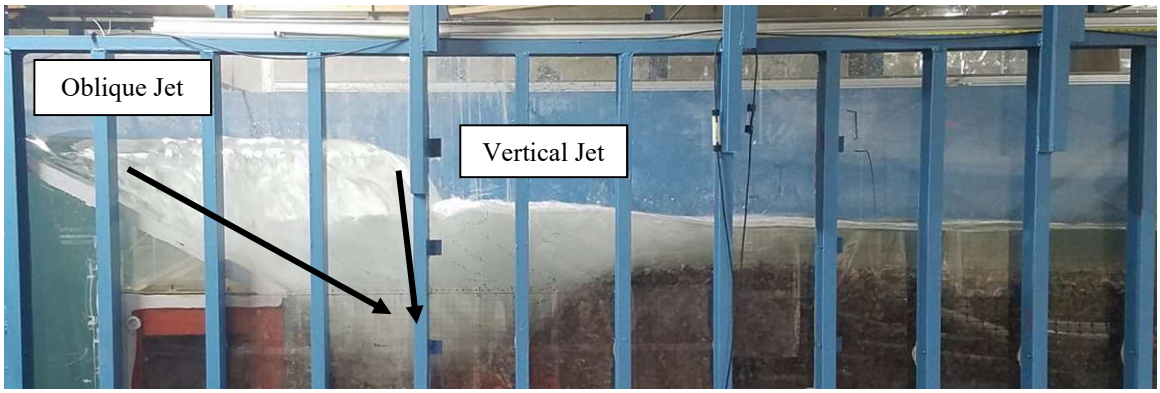

Figure 5. Impinging jets from PK weir.

Local Scour

The hydraulics and geometry of the PK weir result in a peculiar scour pattern characterized by deeper regions interspaced with slightly shallower regions. To illustrate this pattern, Figure 6 presents the scour hole (at equilibrium) for Q=600 L/s (21 cfs) and h_d=0.426 m (16.7 in.). The maximum scour locations occur where the jets issuing from the outlet keys impinge on the downstream riverbed. Minimum scour locations are aligned with the inlet keys.

As gravel movement initiates at the toe of a PK weir, the afore-described pattern is clearly visible as scour deepens and lengthens downstream. Scour morphology is clearly dependent upon the substrate characteristics and hydraulics, specifically the weir geometry, discharge and corresponding headwater and tailwater conditions. The time evolution of local scour at the PK weir with corresponding monitoring locations is shown in Figure 7 for a discharge of 600 L/s (21 cfs) and tailwater depth of 0.426 m (16.7 in.). The configuration without an apron represents a worst-case scenario from this study in terms of scour and illustrates the relevance of considering scour protection measures for field applications.

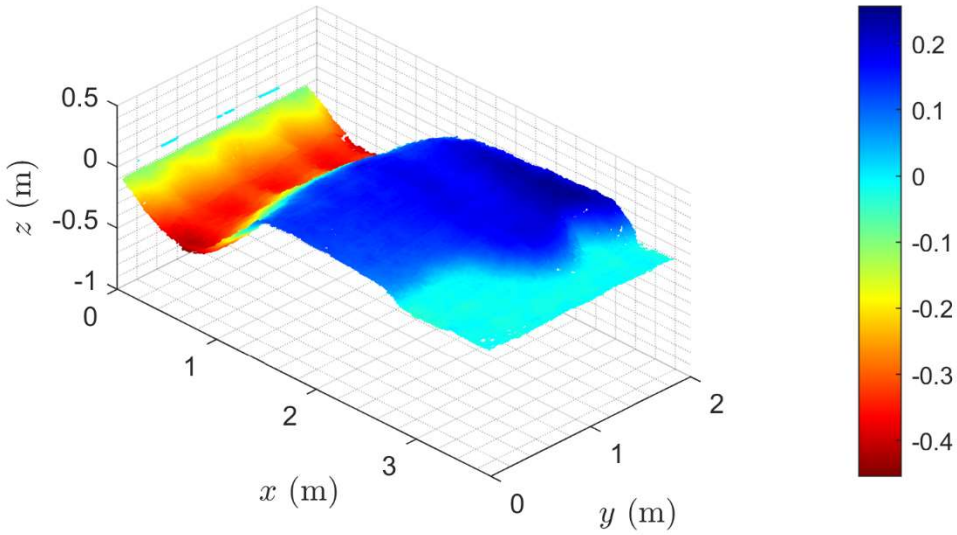

Figure 6. 3-D plot of scour morphology.

Apart from the material tested, a limitation of this study is that experiments did not include routing of any type of storm hydrograph. The maximum scour depths presented herein are at equilibrium and their occurrence is dependent upon sufficient time durations of a specific flow rate. Additional research is needed, particularly field observations, to gain further insight into how maximum scour depths are affected by a storm hydrograph (discharge changing with time). However, the time evolution of local scour presented in Figures 7 and 8 do provide some insights when considering flow hydrographs, peak flow durations, and if the maximum scour depths reported herein might be representative or conservative.

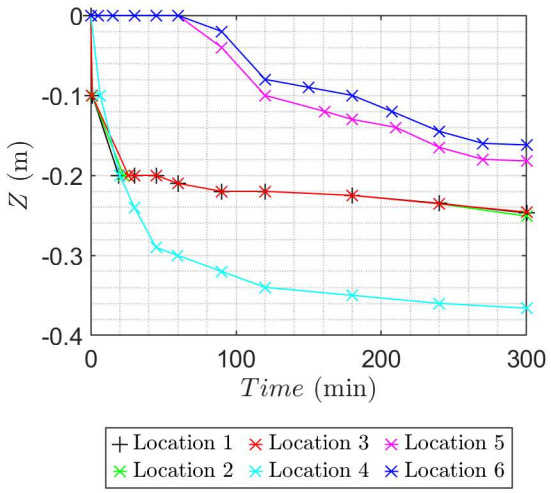

Figure 7. Time evolution of scour depth for 600L/s (21 cfs) and 0.426 m (16.7 in.).

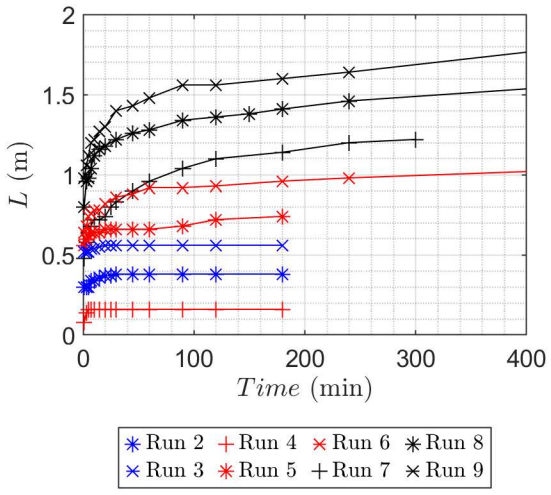

Figure 8. Time evolution of the length of the scour hole.

Scour Protection via a Horizontal Apron

Inclusion of a downstream horizontal apron modifies the scour evolution as the region of impingement at the toe of the PK weir is now protected. Oblique jets from the PK weir outlet keys expand and diffuse over the apron. To consider the effects of apron length on scour depth, three apron lengths were tested in this study with corresponding maximum scour depths presented in Figures 9 through 11, grouped by flow rate. The maximum scour was located separately and the profiles are extracted streamwise along the length of the flume. Also included for comparison are the tests without an apron, or an apron length of 0*P* where *P* references the PK weir height.

Figure 9 represents the maximum scour depths for a flowrate of 150 L/s (5 cfs) with three different tailwater conditions. Figure 9A through 9C represent reference test conditions, and Figure 9D and 9E represents an apron length of 1.5*P* and 2.0*P*, respectively. No scour for the tailwater of 0.417 m (16.4 in.) or for the 2*P* apron was observed. As the tailwater decreased to 0.156 m (6.2 in.) the scour depth increased to approximately 0.18 m (7.1 in.), but when the same conditions are used for an apron size of 1.5*P* the max scour depth was less than 0.05 m (2.0 in.), which is considered negligible.

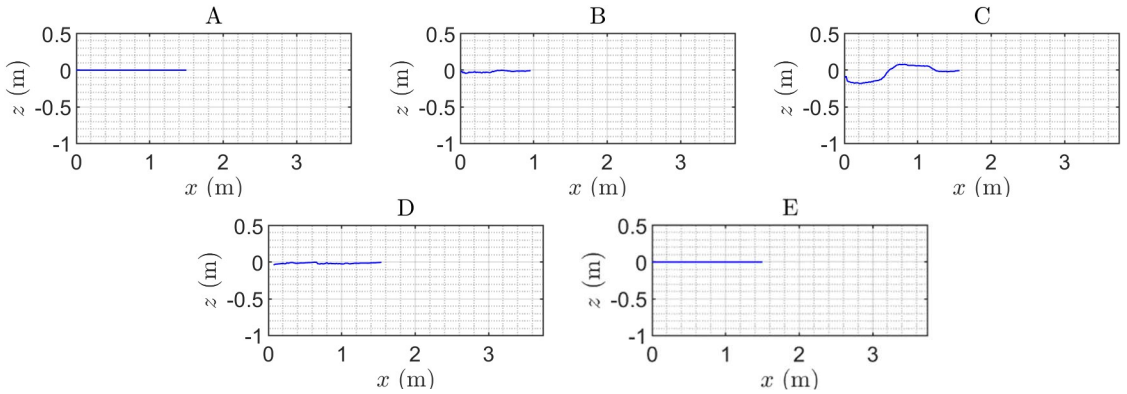

Figure 9. Max scour profiles for Q = 150 L/s (5 cfs) with (A). Apron = 0P, h_d = 0.4165 m (16.4 in.), (B). Apron = 0P, h_d = 0.257 m (10.1 in.), (C) Apron = 0P, h_d = 0.156 m (6.2 in.), (D) Apron = 1.5P, h_d = 0.1 m (3.9 in.), and (E) Apron = 2.0P, h_d = 0.1 m (3.9 in.).

Figure 10 represents maximum scour depths for the intermediate discharge tested herein of 300 L/s (10.5 cfs). Figures 10A through 10C represent scour under reference test conditions but with three varying tailwater elevations. Figures 10D and 10E presents the effects of two apron lengths (1.5P and 2P), which were effective at reducing local scour.

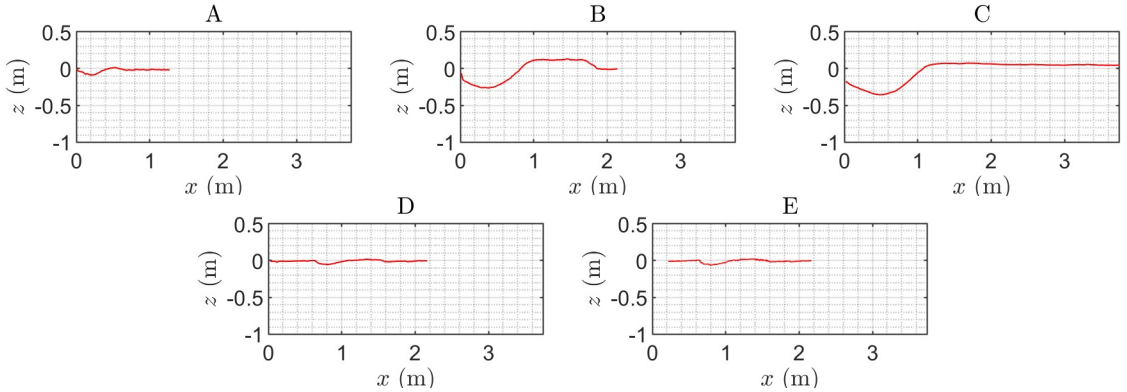

Figure 10. Max scour profiles for Q = 300 L/s (10.5 cfs). A. Apron = 0P, h_d = 0.427 m (16.8 in.), B. Apron = 0P h_d = 0.254 m (10.0 in.), C. Apron = 0P, h_d = 0.174 m (6.9 in.). D. Apron = 1.5P, h_d = 0.172 m (6.8 in.). E. Apron = 1.5P, h_d = 0.146 m (5.7 in.).

Figure 11 represents maximum scour depths for the highest discharge tested herein of 600 L/s (21 cfs). In Figures 11A through 11C the max scour profile under reference test conditions are shown. Scour severity clearly increases as tailwater decreases. Figures 11D and 11E include apron lengths 1.5P and 2.0P, respectively. As shown, the effectiveness of a longer apron is reduced at higher discharges.

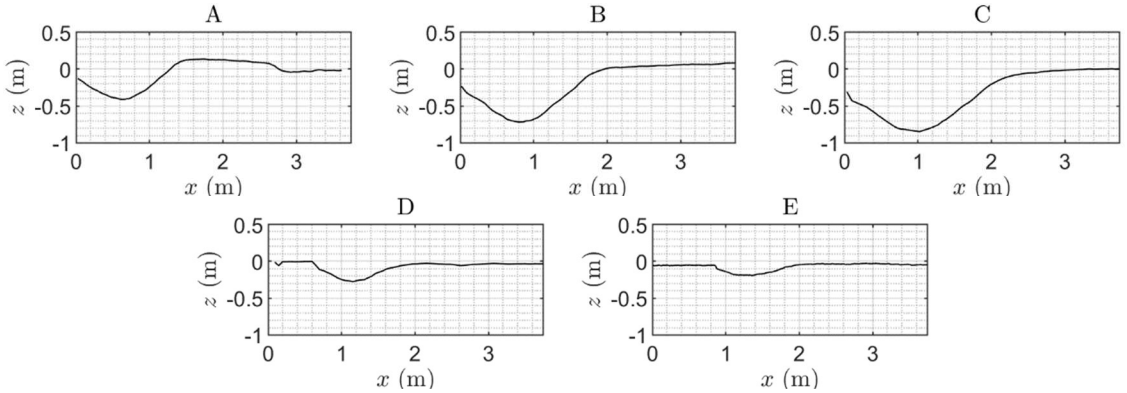

Figure 11. Max scour profiles for Q = 600 L/s (21 cfs). A. Apron = 0P, h_d = 0.426 m (16.8 in.). B. Apron = 0P h_d = 0.280 m (11.0 in.). C. Apron = 0P, h_d = 0.226 m (8.9 in.). D. Apron = 1.5P, h_d = 0.223 m (8.8 in.). E. Apron = 1.5P, h_d = 0.223 m (8.8 in.).

Table 2 summarizes the experimental results from this study including maximum scour depth, the location of maximum scour, and maximum scour length of the hole. Table 2 helps to give definition to Figures 9 through 11 and to help understand the size of the scour hole. Furthermore, Table 2 helps to compare the change in scour between flow rates and tailwater depths.

Table 2. Summary of Experimental Results.

Run #	L_a (m)	Q (L/s)	h_d (m)	Z_{Max} (m)	X_{Max} (m)	L_{Max} (m)
1	0	150	0.417	0.000	0.000	0.000
2	0	150	0.257	-0.042	0.065	0.502
3	0	150	0.156	-0.182	0.215	0.608
4	0	300	0.427	-0.088	0.210	0.442
5	0	300	0.254	-0.263	0.383	0.827
6	0	300	0.174	-0.356	0.486	1.078
7	0	600	0.426	-0.411	0.620	1.220
8	0	600	0.280	-0.717	0.797	1.975
9	0	600	0.226	-0.846	1.023	3.209
10	0.63	150	0.100	-0.038	0.071	0.881
11	0.63	300	0.172	-0.055	0.810	0.459
12	0.63	600	0.223	-0.276	1.155	0.646
13	0.84	300	0.146	-0.072	0.794	0.211
14	0.84	600	0.223	-0.194	1.357	0.436

To highlight the effects of discharge and tailwater on scour features, results are compiled in Figure 12 for reference tests. As expected the scour depth decreases with tailwater, because of the reduction of the shear stress acting on the bed, that scales with $1/(h_d+Z_{Max})$ for all erosive processes. Since it is common to use similitude and scaling laws when comparing laboratory-scale results to field-scale structures, Figures 13 through 15 present non-dimensional ratios of key parameters. Figure 13 correlates the maximum scour depth as a ratio to the total energy head vs a ratio of tailwater depth to the weir height without an apron.

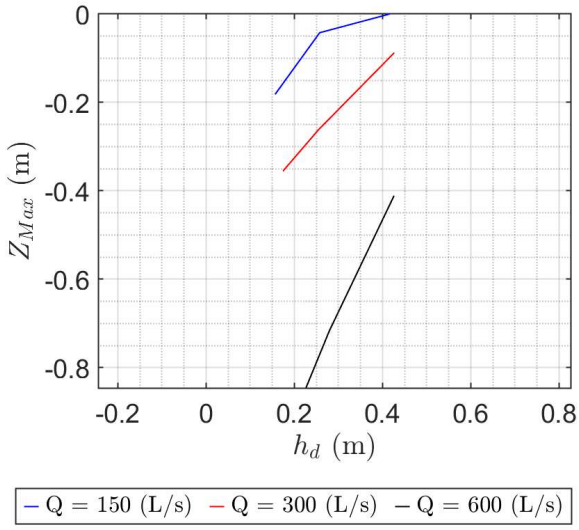

Figure 12. Z_{Max}/h_d for reference tests.

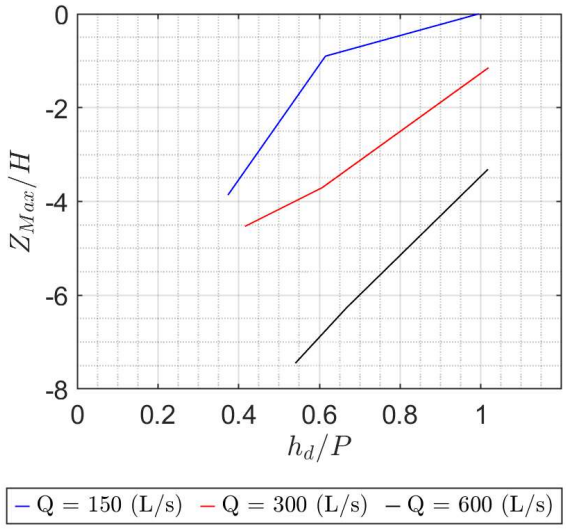

Figure 13. (Z_{max}/H) as function of (h_d/P) for reference tests.

Figure 14 presents max scour over the weir height as a function of downstream tailwater depth divided by the upstream total head. This graph shows that the scour can exceed that of the weir height by almost two times depending on sediment properties, the weir geometry, flow rate, total head, and tailwater conditions. Figure 15 considers maximum scour divided by the median gravel size as a function of tailwater and weir height.

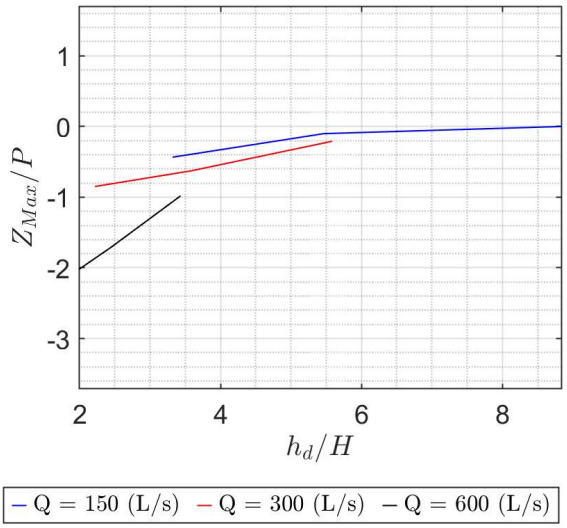

Figure 14. (Z_{max}/P) as function of (h_d/H) for reference tests.

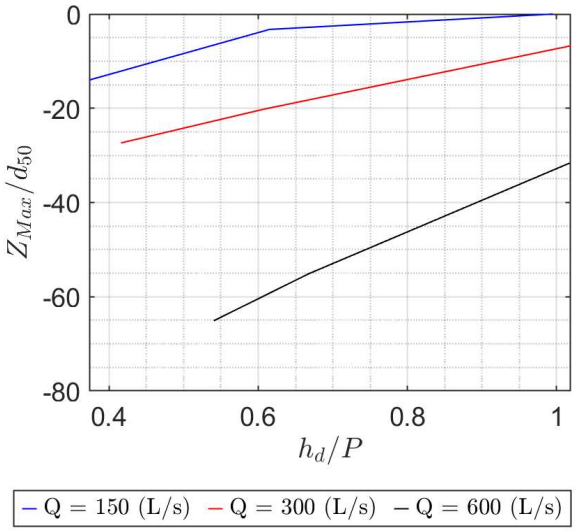

Figure 15. (Z_{max}/d_{50}) as function of (h_d/P) for reference tests.

Figure 16A through 16D present the effects of varying tailwater, flow rate, and apron length on maximum scour depth. Note that the low tailwater condition was the lowest possible tailwater for the corresponding flowrate and its depth is not the same for all tests. The intermediate or medium tailwater refers to the tailwaters approximately 0.28 m (11.0 in.), and high refers to a tailwater depth approximately 0.42 m (16.5 in.). For the reference tests, as the flow rates increase, scour depth and length also increase and as tailwater depths increase scour depth and length decrease. Figure 16B illustrates the effects the aprons have on maximum scour length. Furthermore, the apron transitions the scour jet to a horizontal jet, and hydraulic conditions may still be sufficient to move material and produce a downstream scour hole. From the results it appears that as apron length increases it causes scour to decrease until it reaches a quasi-equilibrium state. Further research would have to be conducted to determine if the addition of longer aprons would entirely discourage scour effects or if the scour reaches a quasi-equilibrium state due to the horizontal jet. Figure 16C through 16D shows how the maximum scour depth is affected with varying flow rates, tailwater conditions, and apron lengths. Figure 16C and 16D share a similar conclusion to that of Figure 16A and 16B but present maximum scour depth.

At locations with erodible streambed materials, it is common to place a cutoff wall at the toe of a structure or apron to prevent scour from undercutting the structure and compromising its foundation. Therefore, the results presented in Figure 16 may be considered when selecting an appropriate cutoff wall depth with or without a horizontal apron.

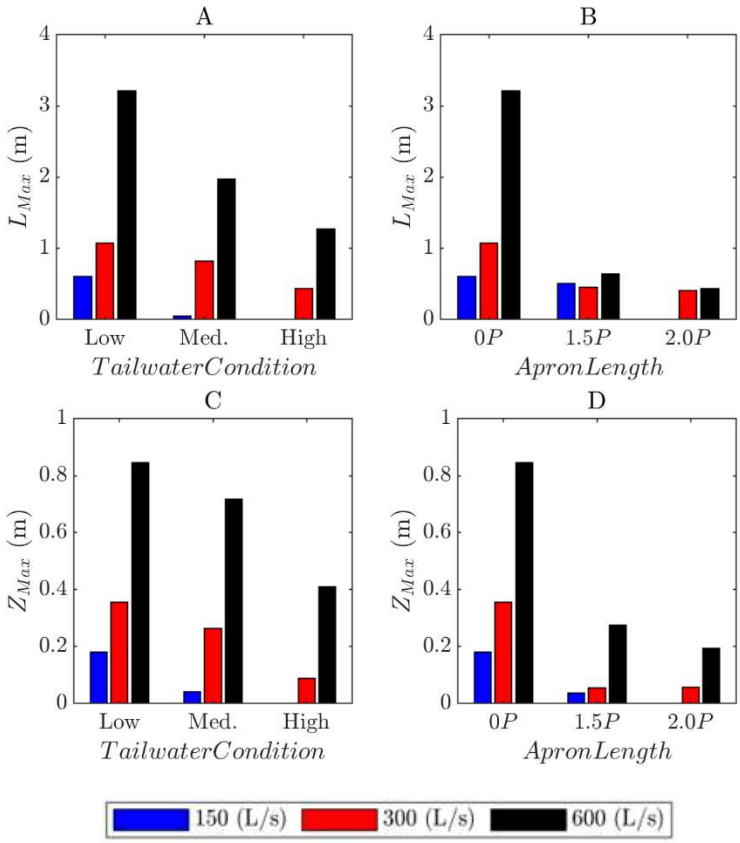

Figure 16A-D. Illustrates scour effects of varying tailwater, flow rates, and apron lengths.

IV. Conclusion

A large-scale multi-phase laboratory study is underway at Utah State University to investigate local scour processes at the toe of a Type A PK weir, including a mitigation option via a downstream apron (of various lengths). The scour phenomenon is complicated and difficult to predict due to the many variables that play a significant role, which include structure geometry, flow characteristics and duration, bed shear stresses, turbulence intensity, and sediment properties. The scour morphology changes depending on the combination of several components. It is concluded that as tailwater increases, the scour length and depth decrease. As tailwater decreases, the scour length and depth increase. It is determined that there is no consistent multiple that an individual can use to accurately estimate the scour depth or length when interpolating between flow rates or tailwater conditions. In an attempt to help practitioners understand the scour effects of non-linear weirs, a graphical approach was taken plotting a combination of energy, median gravel size, maximum scour, weir height, and tailwater conditions.

Furthermore, aprons for run of river structures are essential to minimize local scour. Every run, included in this article, with an apron minimized the maximum scour depth by a minimum factor of three and can range up to four and six, for this gravel size. Though aprons reduce the amount of scour they do not eliminate scour entirely. This article/research shows that the apron deflects the jets and causes local horizontal jet scour downstream of the apron. It is concluded that scour protection drastically minimizes scour depth, but the apron type and lengths investigated does not completely eliminate scour downstream of the apron.

V. Acknowledgment

This study was funded by the State of Utah and the US Geologic Survey, and is in collaboration with the University of California Davis and the University of Pisa, Italy.

VI. References

Abt, S., Ruff, J., Doehring, F. and C.A. Donnell (1987). "Influence of culvert shape on outlet scour." *J. Hydr. Engr.,* 113(3). DOI: 10.1061/(ASCE)0733-9429(1987)113:3(393)

Claudia A & Giampiero S (2006) Scour due to a horizontal turbulent jet: Numerical and experimental investigation, *Journal of Hydraulic Research*, 44:5, 663-673, DOI: 10.1080/00221686.2006.9521715

Crookston, B., Crowley, L., Pfister, M. (2016). Piano Key Weir for Enlargement of the West Fork of Eno River Reservoir. In B. Crookston & B. Tullis (Eds.), Hydraulic Structures and Water System Management. 6th IAHR International Symposium on Hydraulic Structures, Portland, OR, 27-30 June (pp. 447-456). doi:10.15142/T3300628160853 (ISBN 978-1-884575-75-4).

Bombardelli, F. A., Palermo, M., and Pagliara, S. (2018). "Temporal evolution of jet induced scour depth in cohesionless granular beds and the phenomenological theory of turbulence." *Physics of Fluids*, 30(8), 085109, DOI:10.1063/1.5041800.

Bormann, N. E., and Julien, P. Y. (1991). "Scour Downstream of Grade-Control Structures." *J. Hydr. Engrg*, 117(5), 579–594.

Breusers, H.N.C., and Raudkivi, A.J. (1991). *Scouring*. IAHR Hydraulic structures design manual 2. Balkema, Rotterdam, The Netherlands.

Center for Disaster Philanthropy (2019). "2019 Catastrophic River Flooding." https://disasterphilanthropy.org/disaster/2019-u-s-spring-floods/, (Jan. 25, 2020).

Chiew, Y.M., and B.W. Melville. (1986). "Local scour around bridge piers." *Journal of Hydraulic Research.* 25:1, 15-26. DOI: 10.1080/00221688709499285

Crookston, B.M., Erpicum, S., Tullis, B.P. and F. Laugier. (2019). "Hydraulics of Labyrinth and Piano Key Weirs: Prototype Structures and Future Research Needs." *J. Hydr. Engr.* 145(12). https://doi.com/10.1061/(ASCE)HY.1943-7900.0001646 IF: 2.206

D'Agostino, V., and Ferro, V. (2004). "Scour on alluvial bed downstream of grade-control structures." *J. Hydr. Engr.*, 10.1061/(ASCE)0733-9429

"Floods in USA." (n.d.). *FloodList*, http://floodlist.com/america/usa, (Jan. 25, 2020).

Green. C. (2010). "Towards sustainable flood risk management." *Int. J. Disaster Risk Science.* 1(1): 33-43. Doi: 10.3974/j.issn.2095-0055.2010.01.006

Hoffmans, G.J.C.M. and Verheij, H.J. (1997). *Scour manual*. Balkema, Rotterdam, The Netherlands.

Jüstrich, S., Pfister, M. and A.J. Schleiss. (2016). "Mobile river bed scour downstream of a piano key weir." *J. Hydr. Engr.,* 142(11) DOI: 10.1061/(ASCE)HY.1943-7900.0001189

Laursen, E. M. (1952). "Observations on the Nature of Scour." Proceedings of the Fifth Hydraulics Conference, 179–199.

Marsooli, R., Lin, N., Emanuel, k., and K. Feng (2019). "Climate change exacerbates hurricane flood hazards along US Atlantic and Gulf Coasts in spatially varying patterns." *Nature Communications*, 10 (1) DOI: 10.1038/s41467-019-11755-z

"NWS Preliminary US Flood Fatality Statistics." (2020). *National Weather Service*, NOAA, https://www.weather.gov/arx/usflood, (Jan. 25, 2020).

Pfister, M., Jüstrich, S., and Schleiss, A. (2017). "Toe-scour formation at Piano Key Weirs." *Labyrinth and Piano Key Weirs III – PKW 2017*, 147–156. DOI: 10.1201/9781315169064-21

Stein, O.R., Julien, P.Y., and Alonso, C.V. (1993). "Mechanics of jet scour downstream of a headcut." *Journal of Hydraulic Research*, 31(6), 723-738.

Vasquez, V. M., Boyd, M. L., Wolfhope, J. S., and Garnett, R. (2008). "A labyrinth rises in the heart of Texas." Proc., 28th Annual USSD Conf., U.S. Society on Dams, Denver, 813–826.

Wang, L., Melville, B. W., Whittaker, C. N., & Guan, D. (2019, October 10). “Scour Estimation Downstream of Submerged Weirs.", *J. Hydr. Engr.*, 145(12) DOI: 10.1061/(ASCE)HY.1943-7900.0001654

VII. AUTHOR BIOGRAPHIES

Wyatt Lantz is pursuing an MS in Civil Engineering at Utah State University and is currently a graduate researcher at the Utah Water Research Laboratory where he is working on local scour at in-channel structures.

Brian Crookston, PhD, PE is an Assistant Professor at Utah State University and the Utah Water Research Laboratory. Brian’s research and consulting activities are focused on water sustainability and resiliency including: hydraulic structures, fluvial hydraulics, and modeling and technology.

Michele Palermo, PhD, is an Associate Professor at the University of Pisa, Italy. He received a PhD in Civil Engineering Sciences and Techniques in 2009 from the University of Pisa. His primary research interests include local scour phenomena downstream of hydraulic structures, air-water flow properties on rough beds, the design and analysis of eco-friendly structures for river restoration, and physical and numerical modeling.